Pulse Stress Measurement of Controlled Fusion Set by Single Beam Light Holography

O. Yang-Ping, W. Ke-Cheng, P. Li-Hau, X. Xe-Ming
Department of Mechanics,
Huazhong Institute of Technology, Wuhan, Hubie, The People's Republic of China

Abstract—Owing to the strong magnetic field disturbance, it is very difficult to measure in field the pulse stress of the magnetic coil of controlled fusion set by using the resistance wire strain gauge. However, we have succeeded in performing this measurement by using reflection hologram of a single beam light. We have come to the conclusion that the set can operate safely under designed conditions and the fact that it has been running well for three successive years proves the correctness of our conclusion. The principle of holographic interferometry by using a single beam light is put forward and the pulse stress holography equipment and the results of the pulse stress measurement are described. The results of non-destruction test are also given.

1. Basic Principles

In conventional holographic interferometry, it is necessary to strictly isolate the holography system from ambient vibration. This requirement was considerably relaxed after we developed the method of single beam holography [6]. Our method requires that the holographic plate be fixed on the surface of the tested structure. The plate moves together with the structure but it can still show the deformation of the structure. The optic path length difference between the object and reference light is greatly reduced. We can get a good interference pattern even when there is ambient vibration.

a) Reflection Holography Interferometry by a Single Beam

The double-exposure holography interferometry is used for getting the information on deformation. The incident plane light wave is reflected toward the opposite direction since the surface of the structure is coated with orienting reflecting paint as shown in Fig. 1. The intensity of the light on the plate is

$$|H_1|^2 = |O_o e^{iax} + R_o e^{ibx}|^2$$

$$= R_o O_o e^{i(a-b)x} + O_o R_o e^{-i(a-b)x} + O_o^2 + R_o^2$$

$$= R_o^2 + O_o^2 + 2R_o O_o \cos\delta \qquad (1)$$

where $a = k\cos\alpha_1$, $b = -k\cos\alpha_1$, $\delta = ax - bx = k\rho$.

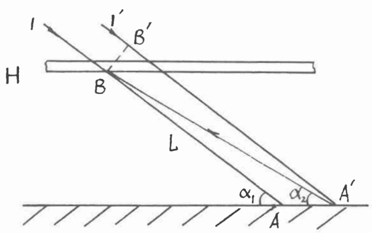

Fig. 1.

After deformation of the structure the second exposure takes place whose value on the plate is written as

$$|H_2|^2 = |O_o e^{i(a+\varepsilon)x} + R_o e^{ibx}|^2$$

$$= R_o O_o e^{i(a+\varepsilon-b)x}$$

$$+ R_o O_o e^{-i(a+\varepsilon-b)x} + O_o^2 + R_o^2$$

$$= O_o^2 + R_o^2 + 2R_o O_o \cos(\delta + \varepsilon x). \qquad (2)$$

where $\varepsilon = -k(\delta\rho)\sin\alpha_1$ when $\delta\alpha$ is small. If we illuminate the hologram with the same light as the reference light, which has undergone double-exposure, development and fixing, the sheet in the fringe plane whose δ is equal to a constant reflects the light wave [6].

$$d\psi = (CR_o \sin\delta \; e^{-i\delta} \, d\delta) O_o e^{iax} .$$

For double-exposure hologram we have

$$d\psi = CR_o O_o e^{iax} \left[\sin k\rho \cdot e^{-ik\rho} + \sin(k + \varepsilon x) \, e^{-ik\rho}\right] dk\rho \tag{3}$$

Integrating eq. (3) over ρ, the deformed and undeformed structures' images that are included in the reflective light wave are

$$\psi_o(x) = C_1 O_o e^{iax} + C_1 O_o e^{i(ax + \varepsilon x)}$$

The intensity is

$$|\psi_o(x)|^2 = 2C_1^2 O_o^2 \left[1 + \cos(\varepsilon x)\right] \tag{4}$$

When x takes the value of $0, \pi, 2\pi, 3\pi, \ldots$ in turn, $|\psi_1(x)|^2$ has the maximum value $4C_1^2 O_o^2$ or zero. The interference pattern showing the deformation of the surface of the structure appears on the observed image. εx represents the phase difference determined by the path length difference ΔL produced by the structure deformation. In Fig. 1, AA' represents the structure surface. The two homogeneous lights 1 and 1' pass through the holographic plate and reach point A(before deformation) and point A'(after deformation). Let AA' = d, AB = L, then

$$\Delta L = A'B' + A'B - 2AB$$

$$= d\cos\alpha_2 + d\cos\alpha_1$$

$$(A'B)^2 = L^2 + d^2 - 2Ld\cos(180^o - \alpha_1) \tag{5}$$

If we want to determine the in-plane displacement when α_1 is small, in general, $\alpha_1 \leqslant 15^o$; we let $\alpha_2 = \alpha_1$. Thus, $\Delta L = 2d\cos\alpha_1$. If $\Delta L = \frac{2n-1}{2}\lambda$, i.e., $d = \frac{2n-1}{4\cos\alpha_1}$, dark fringes appear.

b) <u>Visibility</u>

Because the path length difference by one beam light hologram is very small, the lower coherent laser can be used, and the visibility of the hologram is very high. Fig. 2 shows a hologram taken by one beam light method with multimode ruby laser.

The expression for fringe visibility is determined by

$$V = \frac{I_{max}-I_{min}}{I_{max}+I_{min}} \tag{6}$$

where I_{max} and I_{min} denote the maximum and minimum intensity respectively in the observing plane. When the laser has several frequencies but only the lowest lateral mode, coherence $|\gamma_{1Z}(\tau)|$ can be expressed by time coherence $|\mu_T(\tau)|$:

$$V = \frac{2RO|\mu_T(\tau)|}{R^2 + O^2} \tag{7}$$

where R is the amplitude of reference light and O the amplitude of object light. When R = O, i.e., the amplitude of object light is equal to the reference light, we have

$$V = \mu_T(\tau). \tag{8}$$

In other words, the visibility equals the time coherence. If the time coherence takes its maximum value $|\mu_T(\tau)| = 1$, the visibility V also takes the maximum value, i.e., V = 1. The condition for V = 1 is that the laser operates at single frequency and in single mode or the difference of the travel time between the reference light and object light equals zero, i.e., $\tau = 0$. We fix the holographic plate on the object surface, so $\tau \neq 0$, and $V \neq 1$.

In our case, each pair of object and reference light is in one-to-one correspondence. Therefore, the laser running in high-order lateral mode can be used and a fine hologram is obtained.

Fig. 2.

The QH-1 holographic equipment consists of two portions, a ruby laser, a power supply and a synchronizer. In Fig. 3, a is the He-Ne laser, b the power supply of a, c the ruby laser, d the power supply of c [5] and f the dye case.

A circuit scheme of the ruby laser power supply is shown in Fig. 4, in which A is the main charge circuit, B the sweep circuit and C the automatic control circuit of the voltage.

While the strong pulse current passes through the magnetic coil, a pulse voltage is produced in the measuring coil. At the moment the pulse voltage passes through the zero value, the pulse stress in the magnetic coil reaches the maximum, and the synchronizer shown in Fig. 5 sends out a trigger pulse to make the laser radiate a light pulse. In Fig. 6 the upper curve shows the magnetic signal in the measuring coil, the pulse on the lower one is the light pulse and it corresponds well with the zero value of the magnetic signal in the measuring coil.

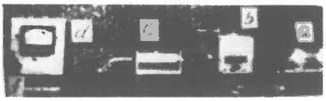

Fig. 3.

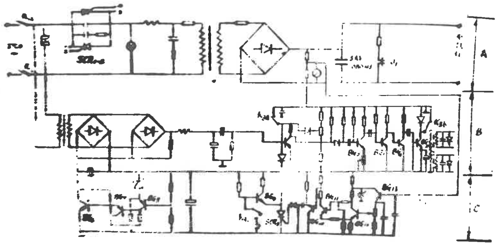

Fig. 4.

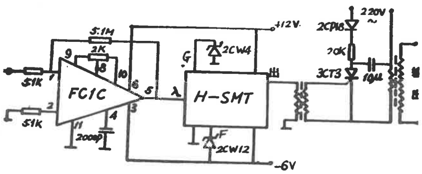

Fig. 5.

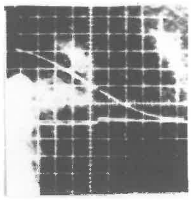

Fig. 6.

2. Measuring Results

The measuring results obtained with QH-1 holographic equipment are listed in Table I.

The measurement is performed at 3 kv voltage and 15,000 gauss of magnetic field. From these results we know that it is safe to operate the controlled fusion set at 4 kv voltage. In this condition, the pulse stresses in the magnetic coil are smaller than the yield strength of the hard copper.

Fir. 7 shows the one beam light hologram of the pulse stresses of the magnetic coil at 2 kv and 3 kv. The photo π_y2kv in Fig. 7 shows clearly the disconnection between the copper wire and the isolation sheet.

Fig. 8 shows the controlled fusion set and the QH-1 holographic equipment.

The measurement data are listed in Table II.

3. Conclusion

The new method of reflecting holographic interferometry by single beam and the QH-1 holographic equipment can be used to measure stresses including the pulse stress in engineering structures. This method has the following advantages:

freedom from vibration isolation that requires only low laser coherence, easy analysis and treatment of fringe data, white light reconstruction, etc.

In the application of holographic interferometry in industry and laboratory work, this method has a bright future.

Ox 2KV

πy 2KV

π/2x 3KV

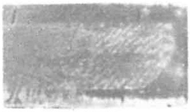

πy 3KV

Fig. 7.

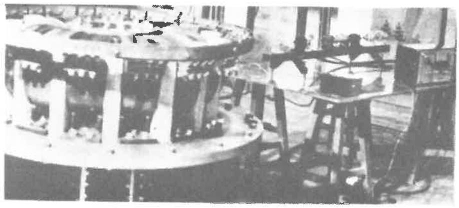

Fig. 8

REFERENCES

1 A.E. Ennos, Measurement of in-plane surface strain by hologram interferometry, J. Sci. Instr. Series 2, Vol. 1, p. 731 (1968).

2 J. Wallach, Holographic strain measurement on a tensile specimen, Proceedings of the Engineering Application of Holography Symposium.

3 Robert J. Collier, Optical Holography, 1971.

4 Ou Yang-ping et al., Some applications in mechanics of holographic interferometry, J. Huazhong Inst. of Tech., Vol. III, No.4, 1975, China.

5 Shanghai Radio Factory No. 13, Electrical system of solid laser, 1972, China.

6 Ou Yang-ping et al., Field applications of holographic interferometry, J. Huazhong Inst. of Tech, Vol. III, No. 4, 1975.

Table I.

position	σ_t(kg/cm^2)	σ_r(kg/cm^2)
π	171	11.3
$\pi/2$	32.2	-32.2
0	16.7	-36.8

Table II.

section	No.	voltage (kv)	fringe No. per 10 mm			strain			stress
			inner	outer	shell	inner	outer	shell	kg/cm^2
π_y	1	2	2	1.5		69.3	51.9		σ_t=155 (3kv)
	2	2	2	1.5		69.3	51.9		
	4	2	2	1.5		69.3	51.9		
	5	2	2	1.5		69.3	51.9		
	7	3	4	3.3	2.5	138.7	112.8	86.7	
	8	3	4	3	2.5	138.7	104	86.7	
π_x	9	2	0.4			13.87			σ_r=10.8 (3kv)
	10	2	0.4			13.87			
	12	3	1			34.63			
	15	3	1			34.63			
	19	3	1			34.63			
$\frac{\pi}{2}y$	35	3	1		0.666	34.63		23.3	σ_r=28.8
	36	3	1.17			40.5			
$\frac{\pi}{2}x$	33	3	1		1.25	34.63		43.4	σ_t=28.8
	34	3	1		i o 1 2.5	34.63		i 34.63 o 86.7	
0_y	23	3	0.666			23.3			σ_t=15.1
0_x	26	3	1		1.5	34.63		23.3	σ_r=33.3
	27	3	1		1.5	34.63		23.3	
	28	2	1/2.5		4			138.7	
	29	2	1/2.5						